Available online at www.sciencedirect.com
SCIENCE DIRECT®
Tectonophysics 420 (2006) 23 – 36
TECTONOPHYSICS
www.elsevier.com/locate/tecto

Constraints from Moho geometry and crustal thickness on the geodynamic origin of the Vrancea Seismogenic Zone (Romania)

Dana M. Mucuta *, Camelia C. Knapp, James H. Knapp

Department of Geological Sciences, University of South Carolina, 701 Sumter Street, Columbia, SC 29208, USA

Received 4 April 2005; received in revised form 28 October 2005; accepted 4 January 2006
Available online 29 March 2006

Abstract

Reprocessing of industry deep seismic reflection data (Ramnicu Sarat and Braila profiles) from the SE Carpathian foreland of Romania provides important new constraints on geodynamic models for the origin of the intermediate depth Vrancea Seismogenic Zone (VSZ). Mantle (70–200 km) earthquakes of the VSZ are characterized by high magnitudes (greater than 6.5), frequent occurrence rates (approximately 25 years), and confinement in a very narrow ($30 \times 70 \times 200\,km^3$) near vertical zone atypical for a Wadati–Benioff plane, located in front of the orogen. These two deep (20 s) seismic reflection profiles (70 km length across the foreland) reveal (1) a high-amplitude, gently east-dipping reflection across most of the section from what we interpret to be the Moho at ~15 s (40–42 km) on the Ramnicu Sarat line to ~16 s (47–48 km) on the Braila line, (2) a thick sedimentary cover increasing in thickness from east (1 s; ~800 m) to west (7.5 s; 14 km), (3) an eastward increase in crustal thickness from 38 km (near VSZ) to ~45 km, (4) seismic and topographic evidence for a newly imaged, possibly seismically active basement fault with a surface offset of 30 m observed on the Ramnicu Sarat line, (5) a lack of notable west-dipping structures in the crust and across the Moho, and (6) variable displacements on Peceneaga–Camena Fault of ~5 km at Moho and ~200 m at the basement–sedimentary cover contact.

These observations appear to argue against recent models for west-dipping subduction of oceanic lithosphere at or in the vicinity of the Vrancea Seismogenic Zone given the lack of west-dipping fabrics in the lower crust and across the crust–mantle boundary. Consequently, one possible explanation for the geodynamic origin of VSZ could be partial delamination of the continental lithosphere in an intra-plate setting along a sub-horizontal lithospheric interface in the Carpathian hinterland that likely involves remnant lithospheric coupling between the crust and uppermost mantle in the foreland.

Keywords: Focsani Basin; Crustal thickness; Moho; Vrancea; Delamination

1. Introduction

One of the most intriguing aspects of the SE Carpathians of Romania is the significant concentration of intermediate depth (down to 220 km) earthquakes in an extremely narrow volume. Two industry deep seismic reflection lines acquired in the Focsani Basin in front of the SE Carpathians bend and to the east of the Vrancea Seismogenic Zone (VSZ) of Romania were reprocessed in an attempt to elucidate the mid to lower crust and uppermost mantle structure some ~50 km eastward from the locus of mantle seismicity. These lines were recorded down to 20 s TWTT in the Focsani

* Corresponding author. Tel.: +1 803 777 3272; fax: +1 803 777 6082.
E-mail address: dmucuta@geol.sc.edu (D.M. Mucuta).

0040-1951/$ - see front matter © 2006 Elsevier B.V. All rights reserved.
doi:10.1016/j.tecto.2006.01.018

Basin as part of the Romanian petroleum exploration activities (Fig. 1).

Under the framework of plate tectonics, mantle earthquakes are understood and explained by subduction of brittle, dense oceanic lithosphere underneath oceanic or continental lithosphere (Isacks et al., 1968), with earthquake hypocenters aligning along Wadati–Benioff planes that mark the subducting slab. Bird, in 1979, proposed delamination as an alternate mechanism for generating mantle earthquakes in an intraplate setting, that do not align on a Wadati–Benioff plane. Delamination is thought to be caused by gravitational instability of over-thickened lithosphere that detaches along a horizontal interface in the lithosphere and sinks into the mantle.

Situated within the 110° bend region of the Southeastern Carpathians, the VSZ represents one of the most active seismic areas in Europe and its yet unclear nature and mechanisms for mantle earthquake generation motivate significant scientific interest. While there have been a number of comprehensive studies on the VSZ and the SE Carpathian foreland (Matenco, 1997; Tarapoanca et al., 2003), these studies have yet to examine the relationship between crustal deformation in front of the Carpathian bend and the VSZ. The foreland Focsani Basin is the site of wide spread low magnitude (<5.5) crustal seismicity and exhibits active subsidence (Radulescu et al., 1996). Documented (Oncescu and Bonjer, 1997) crustal seismicity occurring over a much broader region ($150 \times 200 \times 45\,km^3$) in the SE Carpathian foreland, has not received due attention despite the fact that it is both vertically (~25 km gap) and horizontally (50–100 km) offset eastward from mantle seismicity. The relationship between crustal structures related to basin evolution (especially neo-tectonic structures) to mantle structure and seismicity poses an important and significant geodynamic problem. Foreland deformation at the crustal scale suggests a geometric association with the Vrancea mantle source region, implying a mechanical coupling of the Vrancea seismogenic body with the overlying crust (Knapp et al., 2003).

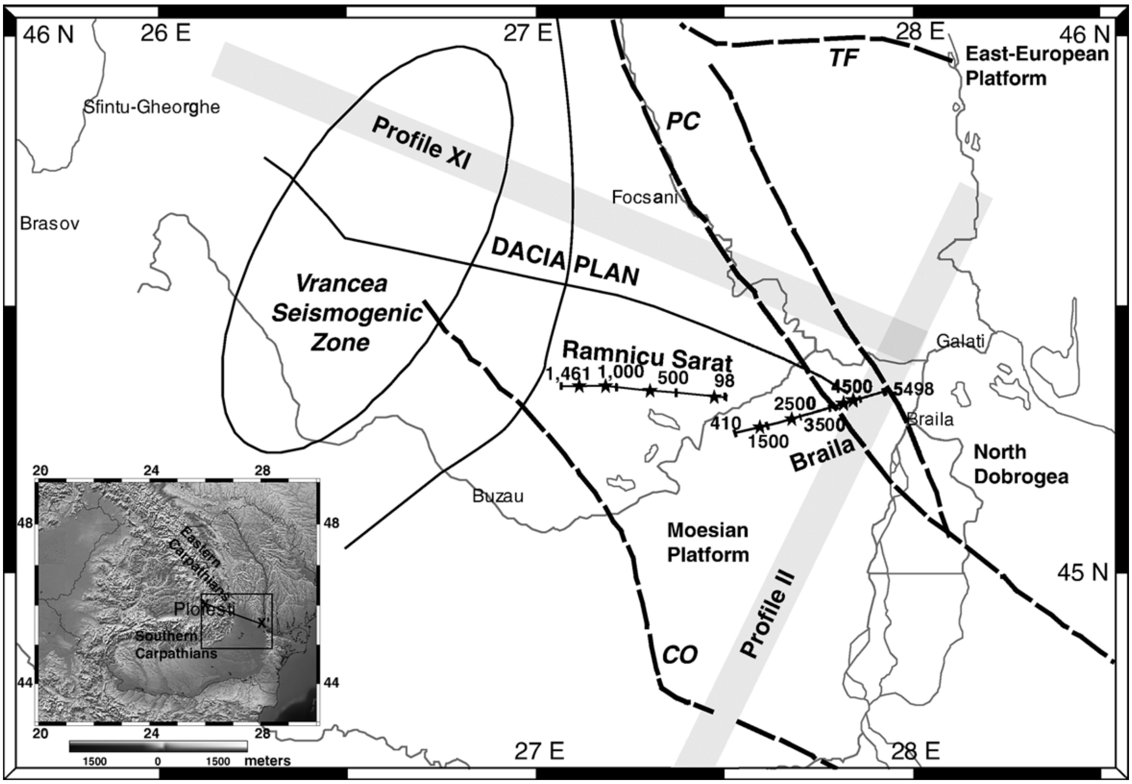

Fig. 1. Location map showing tectonic setting of the Vrancea Seismogenic Zone (VSZ) and location of (1) the Ramnicu Sarat and Braila deep reflection lines, (2) DACIA PLAN seismic reflection profile and (3) refraction profiles XI and II (after Pompilian et al., 1993). CO: Capidava–Ovidiu fault, PC: Peceneaga–Camena fault, TF: Trotus Fault. Inset shows location map of Southern and Eastern Carpathians within the territory of Romania; X–X′ line shows position of cross-section in Fig. 7; box shows location of study area; stars show position of amplitude decay analysis performed in Figs. 2b and 3b; numbers represent CDPs.

2. Geological setting

The Carpathians constitute part of the Alpine–Himalayan orogenic system and formed as a result of the closure of the Tethys Ocean during Mesozoic and Cenozoic time (Burchfiel, 1976; Sandulescu, 1984, 1988; Csontos and Voros, 2004). Within Romania, the Carpathians are traditionally divided into the Southern Carpathians (from the orocline bending of western Romania–eastern Serbia in the west to the bend region), and the Eastern Carpathians (from the bend region in the south to the northern part of the country) (Matenco, 1997). For the purpose of this paper we refer to the SE Carpathians as the 110° bend area at the junction between the Southern and Eastern Carpathians (Fig. 1).

The Eastern Carpathians consist of a complex stack of basement and cover thrust and fold sheets, made up of crystalline basement units and Upper Paleozoic–Mesozoic sediments with a Lower Cretaceous to Tertiary sedimentary cover (Sandulescu, 1984, 1988). Two main periods of compressional deformation are recognized in the Carpathians, one during Late Cretaceous time that was responsible for emplacement of large crystalline thrust sheets now preserved in the Carpathian hinterland, and a second phase during early and middle Miocene time that involved imbrication of a Cretaceous through early Miocene stratigraphic sequence in the Eastern Carpathians (Sandulescu, 1984). This sedimentary section shows a clear affinity with the East European and Moesian continental type of basement on which it now sits (Sandulescu, 1984), and records Miocene-age thin-skinned shortening of as much as 180 km (Ellouz and Roca, 1994). Final nappe emplacement in the Carpathians was mid-Miocene (11–9 Ma) in age, and was followed by continued compression and back thrusting in the Pliocene (Sandulescu, 1984, 1988; Matenco and Bertotti, 2000).

During both Cretaceous and Miocene deformation, the Carpathian orogen developed above a heterogeneous collage of terranes including parts of the East European, West European and Moesian continental crust. Intermediate calc–alkaline volcanic activity is recorded along strike of the orogen, younging progressively from north (with Late Badenian ages 14.3 Ma) to the south and terminating both temporally and spatially in the Persani Mountains around 0.2 Ma (Szakacs et al., 1995; Mason et al., 1998). One of the most peculiar features of the area is the highly arcuate nature of the belt (110°), and the relationship with the locus of present-day mantle seismicity in the absence of any associated volcanism.

Tectonically, the area under consideration (SE Carpathians foreland) involves the East European Platform to the E, the Moesian Platform to the S–SE and the North Dobrogean Orogen to the ESE. A series of crustal scale faults have been identified from old refraction profiles (Enescu et al., 1972; Radulescu et al., 1976, 1979; Radulescu, 1988) such as the Peceneaga–Camena Fault that separates the Moesian Platform from the North-Dobrogea–Scythian block and the Trotus Fault separating the North-Dobrogean Orogen and Scythian Platform from the East European Platform.

2.1. The Focsani Basin

The external part of the Carpathians constitutes the peripheral foreland basin formed during and after Alpine continental collision (Sandulescu, 1984, 1988). The study area encompasses the foreland basin in front of the SE Carpathian bend area delimited by the Intra-Moesian Fault to the south, the Trotus Fault to the north and includes the Focsani Basin (Fig. 1). The SE Carpathian foreland basin is adjacent to the Vrancea area of high seismicity and has a thick (~18 km) Miocene–Quaternary sedimentary cover (Cornea et al., 1981; Tarapoanca et al., 2003) concentric about the Vrancea region. According to Raileanu and Diaconescu (1998) and Hauser et al., (2001) crustal thickness in the Vrancea region (~40 km) is considerably greater than in the surrounding foreland areas (~30 km) and this thickening coincides with the significant accumulation of Neogene–Quaternary sediments in the Focsani Basin (~13 km; Tarapoanca et al., 2003). The basin lies partly on the continental Moesian plate in the SSE and partly on the continental East European Platform in the E and started forming during the later stages of the Cretaceous convergence deriving its sedimentary cover from both platforms (Sandulescu, 1984).

The Focsani Basin, as part of the SE Carpathian foredeep is made up of clastic rocks and evaporites that thicken to the west (Raileanu and Diaconescu, 1997). Still actively subsiding (−2 mm/year) (Radulescu et al., 1996), the basin formed during three orogenic phases, namely the early to middle Miocene, late Miocene and the Pliocene (Sandulescu, 1984, 1988). At its depocenter, the upper 13 km of sedimentary fill of the Focsani Basin are of Tertiary age (Tarapoanca et al, 2003). Previous refraction studies interpreted the Tertiary/Mesozoic boundary at ~9 km, the sedimentary cover/basement contact at ~18 km and the crust–mantle boundary (Moho) at ~42–44 km for the Focsani Basin (Radulescu et al., 1996; Raileanu and Diaconescu, 1998; Raileanu et al., 1994).

Studies on the Focsani Basin present evidence of neo-tectonic activity (Matenco et al., 2003; Tarapoanca

Table 1
Acquisition parameters

Acquisition parameters	Ramnicu Sarat	Braila
Profile name	22-16/93	13-16/94
Profile length	35 km	32 km
Source	Dynamite	Dynamite
Charge size	5 kg/shot	1 kg/shot
Shot point interval	100 m	50 m
Receiver interval	50 m	25 m
Sample rate	2 ms	2 ms
Record length	20 s	20 s
Minimum offset	50 m	25 m
Maximum offset	4800 m	2400 m
Spread configuration	End-on	End-on and split-spread

et al., 2003) with active normal faults trending NNW–SSE, seemingly related to the major Peceneaga–Camena and Trotus crustal faults. According to Matenco and Bertotti (2000), the Peceneaga–Camena–Trotus fault system divides the actively subsiding Moesian Platform from the uplifting pre-Dobrogea–Scythia–East European units. Offsets across the Peceneaga–Camena fault were imaged at crustal scale on previous wide-angle reflection/refraction profiles (Enescu et al., 1972; Radulescu et al., 1976, 1979; Radulescu, 1988) and they appear to vertically displace the Moho by ~5 km (Fig. 5). Other recent normal faults, mostly concentric to the Vrancea zone suggest active deformation of the SE Carpathian foreland (Matenco et al., 2003; Tarapoanca et al., 2003). Shallow, crustal seismic activity is recorded over a broad area, generally with magnitudes <5.5, with focal mechanisms that suggest active convergence in front of the Southeastern Carpathians.

2.2. Vrancea Seismogenic Zone (VSZ)

Despite the numerous studies carried out in this area, the geodynamic setting of the VSZ (Fig. 1) is still the subject of debate. A number of hypotheses (Royden, 1993; Artyushkov et al., 1996; Linzer, 1996, 1998; Girbacea and Frisch, 1998; Wortel and Spakman, 2000; Gvirtzman, 2002; Cloething et al., 2005, Knapp et al., 2005) have been advanced in an attempt to explain the vertical geometry, depth, and restricted lateral extent of mantle seismicity. The debate on the nature of the processes controlling the unusual intermediate depth seismicity, volcanism and surface deformation currently involves three main models:

1. The 'subduction in place' hypothesis (Wortel and Spakman, 2000; Gvirtzman, 2002) assumes subduction of oceanic lithosphere thus accounting for the seismic activity in the Vrancea area but fails to explain the presence of the Neogene age volcanic chain ~150 km towards the west. It also offers a valid explanation for the active subsidence in the Focsani Basin triggered by the pull of the subducting slab still attached to the upper mantle.
2. The 'oceanic slab break-off and retreat' hypothesis (e.g. Linzer, 1996) assumes that a remnant of the Tethys oceanic lithosphere subduction detached from where the youngest volcanic mountains (Persani) are and migrated laterally to its actual position under the VSZ. It accounts for the calc–alkaline volcanic occurrences but the decoupling between the crust and the mantle fails to explain the subsidence of the foreland in front of VSZ as well as the active seismicity in the VSZ.
3. The continental delamination hypothesis assumes that a mass of continental lithosphere (Knapp et al., 2005) is delaminating along a horizontal mid-lithospheric interface and sinking into the mantle thus accounting for the present-day seismicity which does not align along a dipping Wadati–Benioff plane but clusters in a more concentrated volume. The active subsidence of the Focsani Basin would

Table 2
Processing steps

Processing	Parameters
Pre-stack	
Geometry	Straight line geometry
Resample data	4 ms
Top mute and trace edits	
Band-pass filter	Butterworth: 4–8–100–110 Hz
True amplitude recovery	w/ stacking velocities
Trace equalization	0–17000 ms
Air blast attenuation	331 m/s, 150 m/s, 250 m/s, and 840 m/s, 3000 ms window
Datum static corrections	Elevation corrections, 0 m datum and 1600 m/s replacement velocity
Predictive deconvolution	
2D spatial filtering	Mix of 3 traces
Dynamic S/N filtering	
NMO	w/ stacking velocities
CDP stack	24-fold
Post-stack	
F–X Decon (L2 normal adaptive)	
Blend	1:2
Dip scan stack	Dip of 6 traces/s
Dynamic S/N filtering	
Blend	1:2
2D spatial filtering	Mix of 3 traces

indicate that, in this case, the delaminating body is still attached to the crust.

3. Deep seismic reflection data

3.1. Data acquisition and processing

There is quite a considerable volume of geophysical data gathered in the SE Carpathian foreland that has not been until now analyzed with a focus on the deep (15–45 km) structure where crustal seismicity occurs. The long-record petroleum industry seismic reflection profiles used in this study (Fig. 1) were acquired as part of the Romanian hydrocarbon exploration activities with industry parameters (Table 1). Two such profiles with a total length of ~64 km provide an almost continuous image of the SE Carpathian foreland basin in close proximity to the VSZ. The Ramnicu Sarat profile is closest to VSZ and has a W–E orientation while the Braila line is oriented WSW–ENE and continues the Ramnicu Sarat line to the east, with N–S position offset of ~5 km (Fig. 1). The record length of these profiles could theoretically provide information from as deep as 20 s TWTT (~60 km depth assuming a mean crustal velocity of 6 km/s) with adequate data quality, processing techniques and proper velocity analysis. The elevation across the two profiles ranges from 5 m to 120 m. The Ramnicu Sarat seismic profile was initially processed for industrial purpose with a focus on the shallow, sedimentary section down to 6 s (12 km) (Raileanu and Diaconescu, 1998) while there is no published literature on the Braila line. The main target of this study was the imaging of Moho and crustal structures that could provide constraints for the geodynamic processes governing the neighboring Vrancea area. Of specific interest was the imaging of potential dipping, continuous reflectors from the upper crust to the upper mantle truncating the Moho, which would favor or disprove the subduction model. For the purpose of reprocessing, the data were de-sampled to 4 ms and processed using the ProMAX seismic processing package.

Processing of data targeted the enhancement of signal from longer travel times while preserving the

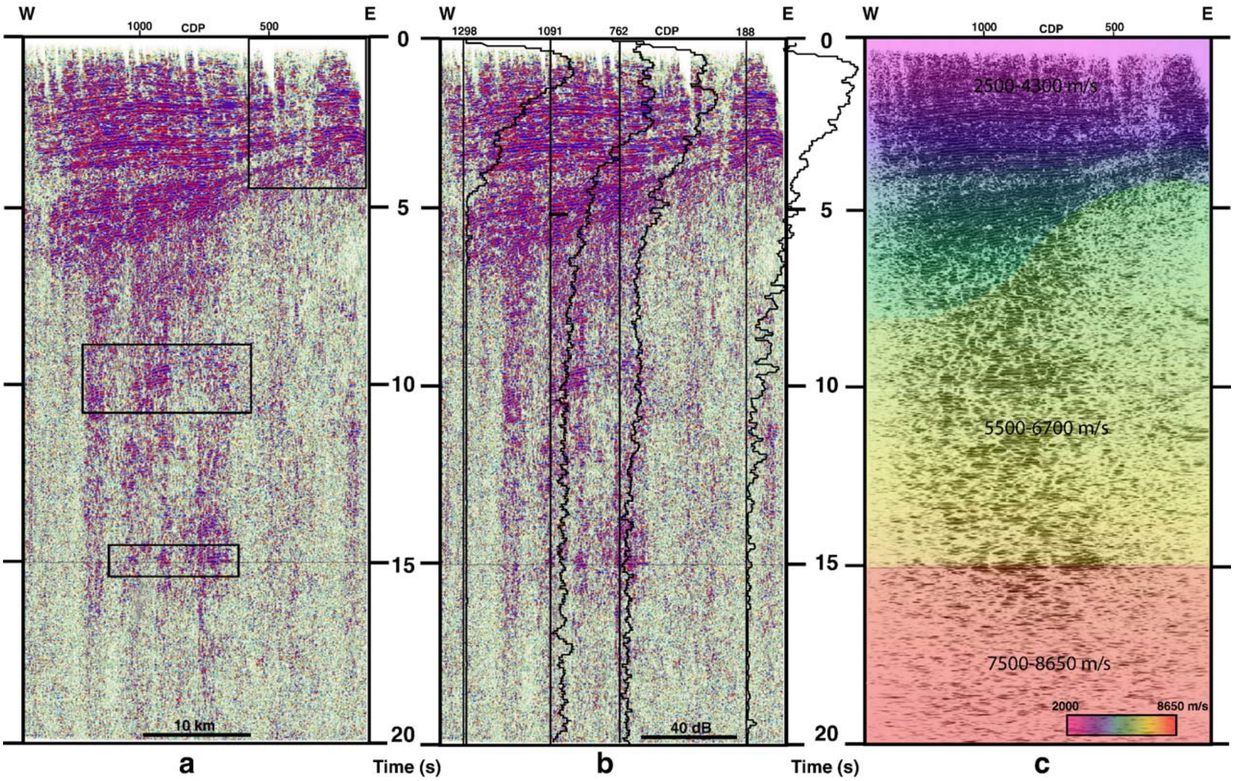

Fig. 2. Reprocessed Ramnicu Sarat profile showing: a) time section down to 20 s TWTT, b) amplitude decay curves superimposed on the time stack, and c) interval velocity model superimposed on the migrated time section, showing collapse of mid-crust arcuate features identified as diffractions. Section is displayed at 1 : 1 scale for a mean crustal velocity of 6 km/sec. Boxes show locations of Fig. 4a, b and e (mid-crust arcuate diffraction features).

information in the shallow section. Air blast attenuation and coherency filters significantly improved the quality of the shot gathers and provided better correlation from shot to shot. Ground-roll was visible on most shots on the Ramnicu Sarat line and to a less extent on the Braila line thus processing of data targeted the removal of unwanted energy in order to enhance the energy hidden by ground-roll. Stacking velocities inferred from detailed velocity analysis performed on the filtered shots were used for normal-moveout (NMO) correction and stacking (24-fold). Refraction velocities from two international refraction profiles crossing the study area (Figs. 1 and 5) (Enescu et al., 1972) were used to constrain velocities at longer travel times on the Braila line. Elevation static corrections were applied in order to align the seismic traces to the same datum (0 m) and a replacement velocity of 1600 m/s from short refraction profiling was used in order to perform this correction. Predictive deconvolution (Taner et al., 1991) was useful for removal of multiple energy and spiking deconvolution was used for collapse of the wavelet and sharpening of the reflectors. The dip scan stack filtering (Stoffa et al., 1981) was used to increase coherency pre- and post-stack by weighing the traces along a given dip along with enhancement 2D spatial filters. The stacks were blended with different weights to avoid an over-filtered and mixed image of the final time sections. Processing steps are listed in Table 2.

The resulting time sections (Figs. 2a and 3a) were migrated using the finite-differences technique (Yilmaz, 1987) to account for vertically and laterally variable interval velocities (converted from stacking velocities). Images of the migrated time sections superimposed on the interval velocity fields (Figs. 2c and 3c) are provided in order to show the accuracy of the velocity picks and also the collapse of diffractions for accurate interpretation. The Ramnicu Sarat and Braila profiles differ in their receiver and shot-point interval as well as charge size thus leading to some noticeable differences in the aspect of the reflection character. In addition, there is a gap of approximately 8 km in the middle of the Braila line where there are no data. The Braila profile was recorded with an end-on spread configuration for the western half of the line and with split-spread for the eastern half; however no information is available to explain this change.

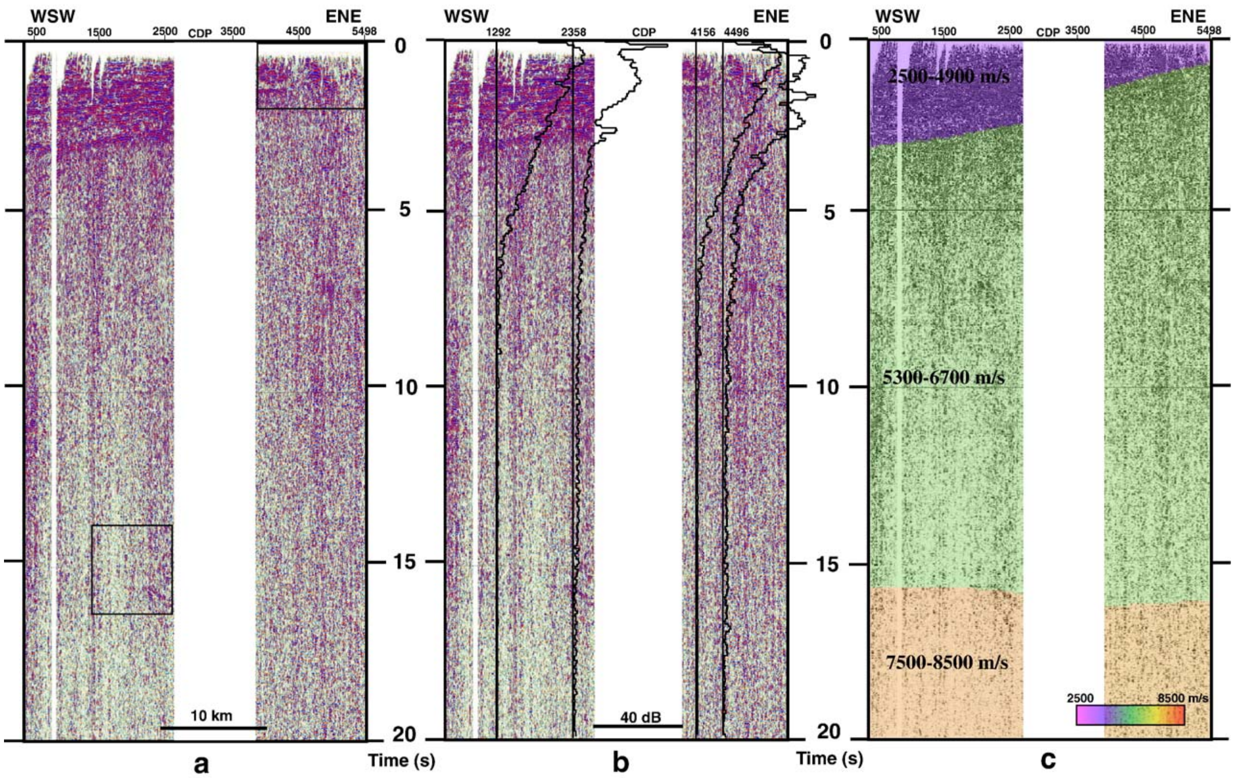

Fig. 3. Braila profile showing: a) time section down to 20 s TWTT, b) amplitude decay curves superimposed on the time stack, and c) interval velocity model superimposed on the migrated time section. White band represents area of no data. Section is presented at 1 : 1 scale for a mean crustal velocity of 6 km/sec. Boxes show locations of Fig. 4c and d.

Moreover, the shorter offset (of 2400 m) on the Braila line may be responsible for the poorer imaging below ~4 s, not allowing for adequate NMO, while the maximum offset of 4800 m on the Ramnicu Sarat line allowed for a good reflection image along the entire length of the trace.

3.2. Amplitude decay analysis

Amplitude decay analysis has proven to be a useful technique to determine seismic signal penetration with depth and to evaluate whether lack of reflectivity is due to poor signal penetration or has geological causes (Barnes, 1994; Knapp et al. 2004). The dynamite charge was of 5 kg/shot for the Ramnicu Sarat line and 1 kg/shot for the Braila line; thus, the smaller charge may also explain the poorer reflectivity from longer travel times on the Braila profile. The analysis was performed on all of the edited but unfiltered and unprocessed CDP gathers in order to obtain a realistic estimate of the maximum depth of signal penetration.

The amplitude decay curves show sufficient energy penetration down to longer travel times on the Ramnicu Sarat line (Fig. 2b), suggesting that there is potential information that could be imaged from depths as high as 60 km whilst lack of signal at some points may suggest geological causes. Consequently, different processing techniques (Table 2) were employed and aimed at enhancing the reflectors at larger depths in order to enable an adequate imaging of structures down to 15 s and beyond, where adequate seismic energy was present.

Depending on their locations, the four amplitude decay curves superimposed on the Ramnicu Sarat time section (Fig. 2b) present different characteristics. The amplitude decay curve for CDP 1298 shows loss of energy by 5 s possibly explaining the lack of reflectivity from 15 s TWTT, while CDP 188 curve shows

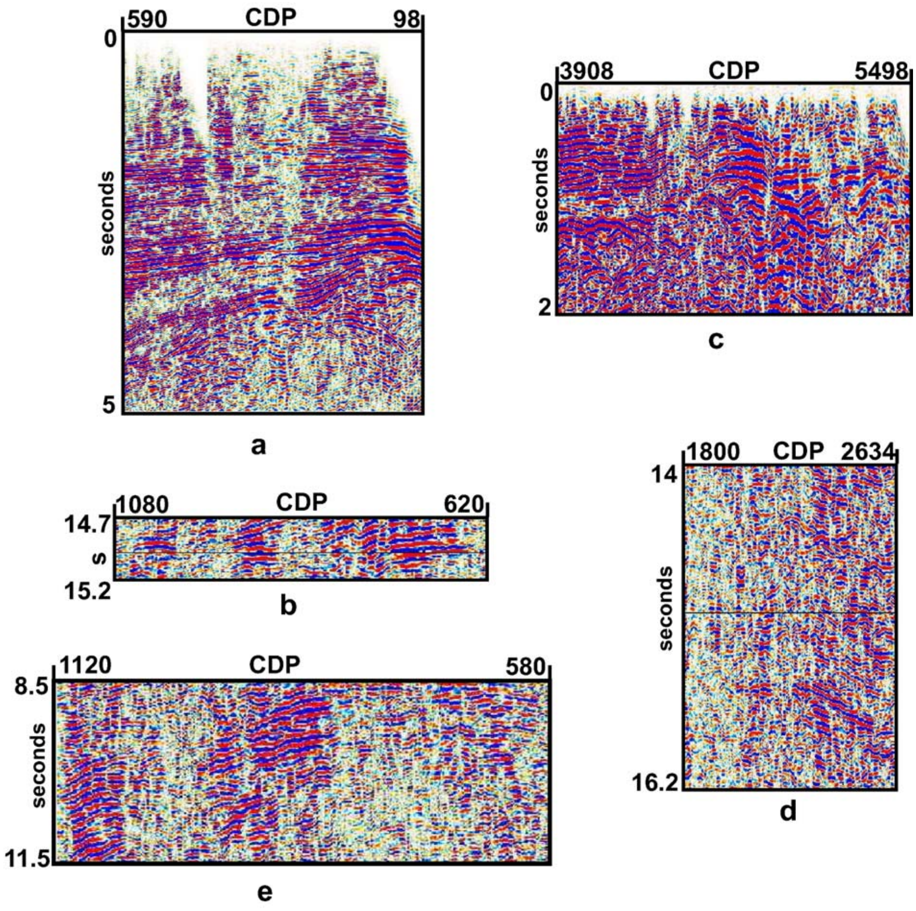

Fig. 4. Enlarged images of: a) Ramnicu Sarat E basement cutting Focsani Fault; b) Ramnicu Sarat 15 s reflector (Moho) approximately 12 km long; c) Braila basement cutting faults to the ENE associated with the Peceneaga–Camena fault zone; d) Braila 15.6 s reflector and e) Ramnicu Sarat mid-crust arcuate diffractions.

amplitudes decaying down to 12 s, in this case lack of reflectivity being attributed to the geologic structure. CDPs 1091 and 762 curves have similar patterns, with amplitudes decaying down to ~16 s, implying good signal penetration with depth, and thus making the imaged deep reflectivity reliable.

The Braila line amplitude decay analysis (Fig. 3b) shows generally poorer signal penetration with depth. The superimposed amplitude decay curves typically exhibit loss of signal by ~8 s, such as for CDPs 1292 and 4156, coinciding with lack of reflectivity from longer travel times. However, loss of seismic energy occurs at later travel times (~16 s) for CDPs 2358 and 4496, substantiated by the 15.6 s dipping reflector on CDP 2358 and some coherent reflectivity at ~10 s on CDP 4496. For both profiles, the maximum logarithmic amplitude of the amplitude decay curves was ~40 dB.

The calculated amplitude decay curves determined the limitation of seismic energy penetration with depth for the two lines emphasizing the importance of adequate dynamite charge and geological structure. While the strong, horizontal, 15 s reflector on the Ramnicu Sarat line (Figs. 2 and 4b) distinctly marks good seismic energy at this long travel time, there is less clear evidence for coherent seismic energy reflection energy below ~4 s on the Braila line.

3.3. Observations

The Ramnicu Sarat time section presented here (Fig. 2a) shows very good coherent reflectivity down to ~15 s making it possible to draw some pertinent conclusions about the geodynamic setting of this area. Possibly due to poorer data quality and lack of information within CDP range 2600–3700, the Braila profile was never published previously (Fig. 3a).

The Ramnicu Sarat time section (Fig. 2a) shows: (1) continuous, parallel, horizontal reflectors in the sedimentary section down to ~8.5 s (W) shallowing to ~3.5 s (E); (2) shorter, coherent reflectors (CDPs 1300–500) in the upper and middle crust (9–13 s TWTT); (3) arcuate diffracted energy (CDPs 1200–800) at ~9–11 s (Fig. 4e); (4) a high-amplitude, horizontal reflector across most of the section at ~15 s (CDPs 1300–500) (Figs. 2 and 4b); and (5) evidence for a newly imaged, possibly seismically active fault with a surface offset of 30 m (Fig. 4a). The interval velocities superimposed on the migrated time section (Fig. 2c) show velocity increasing with depth and the main velocity boundaries: sedimentary cover-basement at ~8.5 s (W) and ~3.5 s (E) with a velocity increase from ~4300 m/s to ~5500 m/s and the Moho or the inferred crust–mantle boundary at ~15 s with a velocity jump from ~6700 m/s to ~7500 m/s. Mohorovicic (1910) identified the crust–

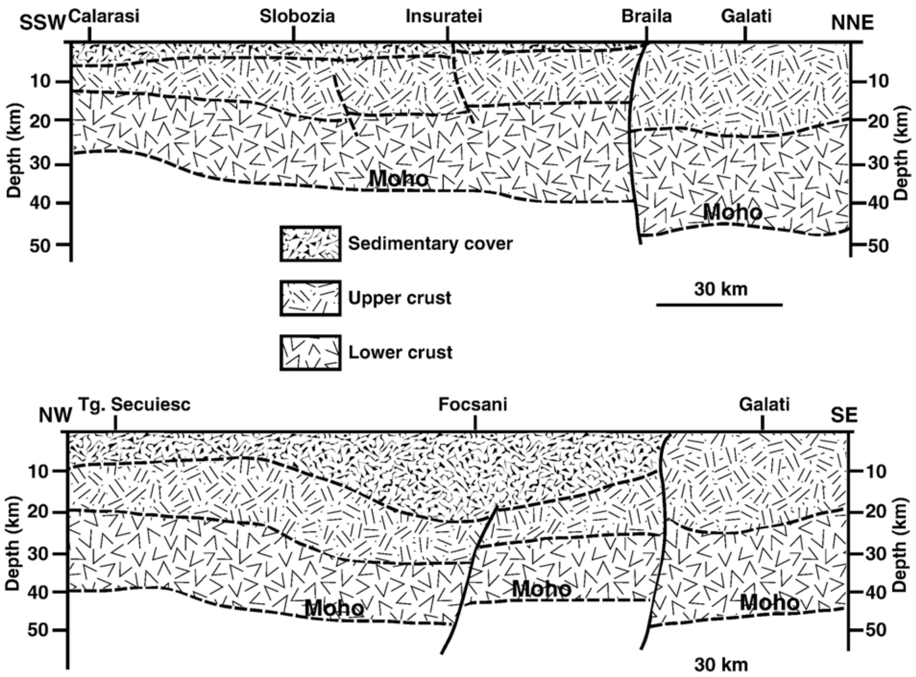

Fig. 5. Adapted cross-sections of the seismic refraction profiles XI (Tg. Secuiesc–Galati) and II (Galati–Calarasi) showing the inferred position of the Moho along with Moho offsets caused by the crustal-scale fault Peceneaga–Camena (modified after Pompilian et al., 1993).

mantle boundary as a velocity increase from ~6500 m/s to ~7900 m/s as inferred from seismological data. Short sub-horizontal coherent events (9–13 s TWTT) characterize the upper and middle crust while the Moho is marked by an approximately 12-km-long sub-horizontal reflector at ~15 s, with the crust being more reflective on the western and middle portion and transparent on the eastern end. As mentioned, the Moho is seen as an abrupt velocity step, marked by a sharp high-amplitude reflector rather than a gradual transition zone. The mid crust arcuate features were distinguished as diffractions following time migration of stacked data (Fig. 2c).

Braila reprocessed time section (Fig. 3a) shows: (1) continuous reflectors in the sedimentary section down to ~3.5 s (W) shallowing to ~0.8 s (E); (2) diffracted energy at the base of the sediments indicated by arcuate features; (3) some coherent reflectivity ~10–12.5 s on the western side; (4) a short (CDPs 1800–2600), dipping reflector at ~15.6 s (Fig. 4d); and (5) a series of basement cutting faults (CDPs 4300–5400) (Fig. 4c). Interval velocities superimposed on migrated time

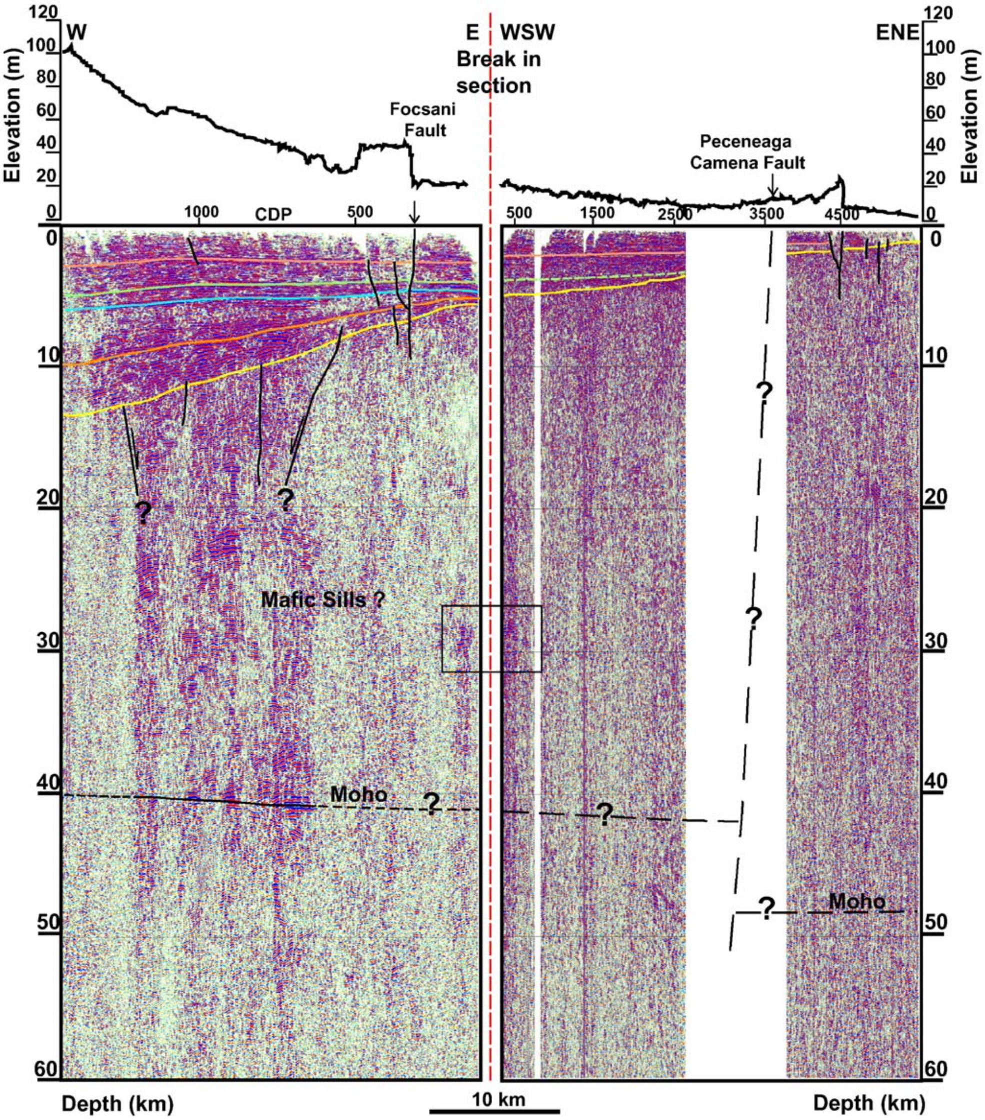

Fig. 6. Interpreted depth section of combined Ramnicu Sarat and Braila profiles (break in section indicated). Sedimentary horizons color-coded as follows: pink (Top Dacian, ~3.5 Ma), green (Top Sarmatian, ~10.5 Ma), blue (Intra Sarmatian, ~11.5 Ma), orange (platform top, senso Matenco), yellow (sedimentary cover-basement contact). Elevations are plotted on top, ranging from 110 m to 5 m. Arrows show the location of the newly identified Focsani Fault and the inferred position of the Peceneaga–Camena Fault. Black vertical lines represent other interpreted faults. Black box shows continuity of reflectivity from one section to another at mid-crustal level. Section is displayed at 1 : 1 scale.

section (Fig. 3c) show a similar velocity increase with depth and the main velocity boundaries: sedimentary cover-basement at ~3.5 s (W) and ~0.8 s (E), and the inferred Moho at ~15 s. Due to the poor reflectivity at longer travel times, the Moho depth was constrained by previously recorded seismic refraction data in the SE Carpathian foreland (Fig. 5; Pompilian et al., 1993). The very shallow basement on the eastern side (Fig. 4c) at 0.8 s is indicated by the geology to be the Dobrogean basement (Sandulescu, 1984) and marks the eastern termination of the Focsani Basin. Migration of data removed diffracted energy at the top of the basement but maintained the dipping signature of the 15.6 s reflector. The two depth images (Fig. 6) were obtained by converting the time stacks to depth using interval velocities derived from the stacking velocities as well as refraction velocities from seismic experiments performed in the area (Radulescu et al., 1976; Hauser et al, 2001; Raileanu et al., 2005).

4. Interpretation and discussion

For interpretation purposes, the two depth images obtained by converting the time stacks to depth are displayed side by side (Fig. 6) in order to obtain a longer (~70 km) cross-section over the study area. In doing this, the authors looked for a better correlation of events and thus a more reliable interpretation. It can be observed that there is good continuity between the two lines with the sedimentary section becoming thicker from east (~0.8 km) to the west (~14 km). There is also good correlation at mid-crustal level between the two lines, with a package of reflectors at ~20 km and 28–30 km on the Ramnicu Sarat line being easily followed at the same depths on the Braila line (box, Fig. 6).

The cross-section presented here (Fig. 6) shows: (1) a thick sedimentary cover increasing in thickness from 0.8 km (E) to ~14 km (W) towards the VSZ; (2) the inferred position of an extensional Mesozoic or older graben (Panea et al., 2005) possibly rotated during the Tertiary subsidence of the basin which may explain the strong mid-crustal reflectivity through magmatic intrusions, on the western side of the cross-section; (3) an eastward increase in crustal thickness from ~40 km in the vicinity of the VSZ (W) to 48 km (E); (4) a high-amplitude eastward-dipping reflection from ~40 km (W) to ~42 km (E) interpreted to be the Moho on the Ramnicu Sarat profile; (5) seismic and topographic evidence for a newly imaged, possibly seismically active basement fault with a surface offset of 30 m observed on the Ramnicu Sarat line (CDPs 250–300); (6) strong fracturing of the basement by normal faults on the Braila line; and (7) the notable absence of west-dipping fabrics in the crust and across the Moho, as would be expected from westward subduction. Though the east-dipping Moho (40–42 km) on the Ramnicu Sarat line is easily observed on the seismic section, the depth and geometry of the Moho on the Braila line is only partially supported by the data presented and is mostly constrained from refraction results.

The imaged sedimentary section of ~14 km (W) (Fig. 6) falls in the maximum 18 km of sediments considered to be the thickness of the Focsani Basin at its deepest point further to the west (Radulescu et al., 1979). Age control on the sedimentary sequence (Ramnicu Sarat line) was provided by Matenco (1997) from well data, and the top of the basement is clearly imaged across the entire cross-section. The topographic offset of ~30 m on the eastern end of the Ramnicu Sarat section is interpreted as a basement-cutting fault due to the break and different character of the reflectors, and appears to propagate all the way to the surface. We named this recent fault the Focsani Fault due to its vicinity of the city of Focsani. Normal faults at the basement level were imaged, without continuation to the surface, suggest extension and possible relation with a Mesozoic or older graben in the middle crust that was imaged as a series of parallel, layered reflectors. On the easternmost end of the cross-section we infer the position of a basement cutting series of flower-structure normal faults (Fig. 4c), confirmed by the very different character of the reflectors, that could be branches of the crustal scale (Radulescu et al., 1976) Peceneaga–Camena fault. Based on the position of the Braila profile in correlation with data from international seismic refraction profiles II and XI (Figs. 1 and 5) (Radulescu et al., 1979; Pompilian et al., 1993) and seismic reflection profile DACIA PLAN (Panea et al., 2005), the map projection of the Peceneaga–Camena fault is determined to be in the no-data portion of the profile (CDP range 2600–3700) as shown in Fig. 6.

The horizontal, mid-crustal reflectivity (22–32 km) could possibly be interpreted as caused by magmatic injections during the Mesozoic extension though the older Romanian literature refers to it as the Conrad discontinuity, supposedly marking the transition from the upper crustal layer (granitic) to the lower crustal layer (basaltic) (Enescu et al., 1972; Pompilian et al., 1993). The extensional rift structure interpretation is also supported by results of the DACIA PLAN reflection profile carried out in 2001 (Panea et al., 2005) traversing the internal East Carpathians, the SE

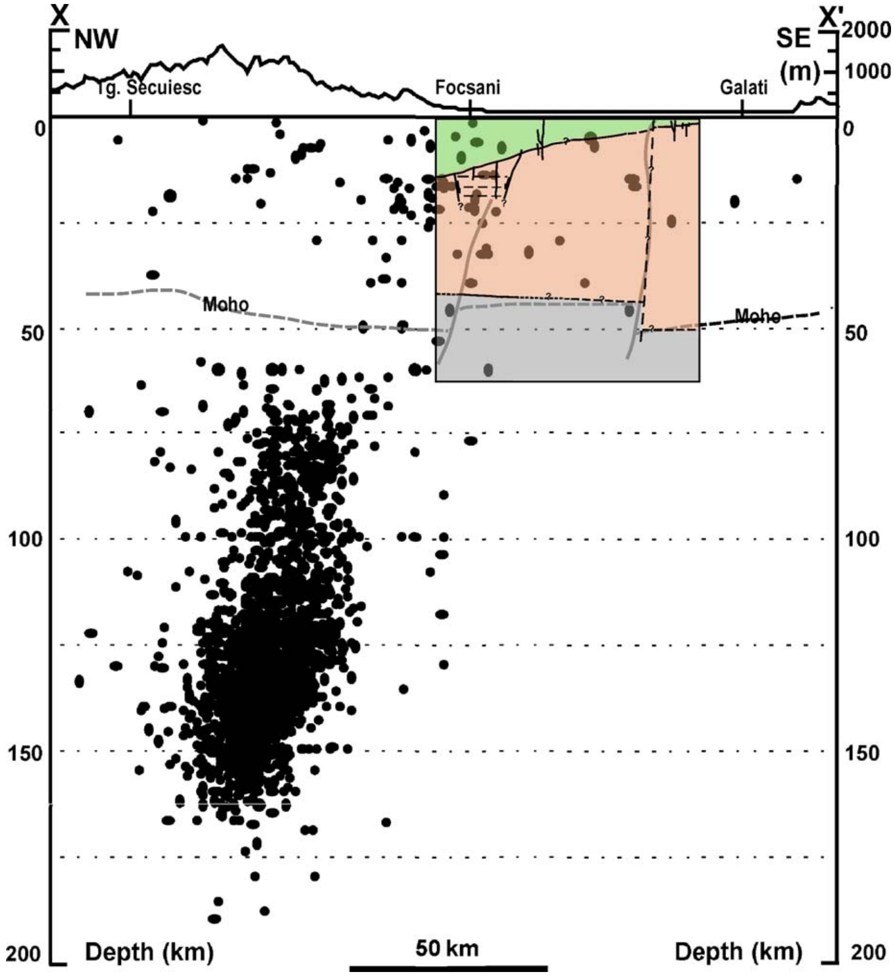

Fig. 7. Interpreted depth model integrated on lithosphere-scale cross-section along NW–SE transect (X–X′ line in Fig. 1 inset). VSZ hypocenters shown by dots, Moho boundary from refraction survey (Pompilian et al., 1993) (gray dashed line) and topography across transect. Model shows sedimentary section (green), crystalline crust (pink) and mantle lithosphere (gray); the inferred Mesozoic or older graben is shown with dashed dark lines.

Carpathians and Focsani Basin on a WNW–ESE orientation (Fig. 1).

The crust–mantle boundary is clearly imaged on the Ramnicu Sarat profile gently dipping eastward from 40 km to 42 km depth, supported by the amplitude decay analysis and the different reflective character (lack of reflectivity) below 16 s, while on the Braila line constraints from the existing refraction lines, especially refraction profile XI (Fig. 5), were used in conjunction with our observations to infer Moho depths of 45–48 km towards the east, and offsets of ~5 km (Pompilian et al., 1993) along the interpreted position of the Peceneaga–Camena fault (Figs. 6 and 7). The deep (15.6 s) short, dipping reflector imaged on the Braila line is interpreted to be a mantle reflector.

The imaged seismic lines are integrated on a lithospheric-scale cross-section (Fig. 7) oriented NW–SE, across the SE Carpathian orogen and the foreland and results from refraction line XI at the Moho level are superimposed on the interpreted depth section. Our data substantiated the Peceneaga–Camena Fault with offsets in the sedimentary cover-basement contact but no evidence was found for the Capidava–Ovidiu Fault.

The eastward-dipping geometry of the Moho in the close proximity to VSZ and the absence of west-dipping crustal fabrics render subduction of oceanic lithosphere an unlikely explanation for Vrancea seismicity. Another important constraint is the thickening of the crystalline crust from W to E, away from VSZ, which is exactly the opposite from what would be expected in the presence of subduction. Given its proximity to the fold and thrust belt, one would expect thickening of the crust towards the Vrancea zone not away from it, in order to account for the orogenic root and elevated topography, quite the contrary to what our study revealed.

The thickness of the sediments suggests a higher accumulation rate during the subsidence of the basin due to the bending of the lithosphere under the load. The dramatic thinning of the crystalline crust in the proximity of the Vrancea area could be associated with the failed Mesozoic or older rift graben and the thick sedimentary cover due to ongoing convergence, with the Moesian platform crust of continental thickness (~45 km) and affinity.

5. Conclusions

Two deep (20 s, 60 km) seismic reflection profiles (Ramnicu Sarat and Braila) were acquired as part of the petroleum exploration activities in the deep Focsani Basin and were processed here with a target on the lower crust–upper mantle structure in order to provide constraints on the geodynamic setting of the Vrancea Seismogenic Zone. This paper attempts to verify the validity of the "subduction in place" hypothesis, proposed by many authors as responsible for the intermediate-depth seismicity of the Vrancea Area, with regional geologic implications. Situated in the vicinity (~50 km) of VSZ, these two lines offer a combined ~70-km-long, 60-km-deep image of the crust and uppermost mantle in the SE Carpathian foreland basin, providing a window through the crust and uppermost mantle in the close proximity of the seismogenic zone.

The seismic reflection data presented here were integrated with previously acquired refraction (Radulescu et al., 1979; Pompilian et al., 1993; Raileanu et al., 2005) and reflection profiles in the study area (Panea et al., 2005), as well as with and other geologic studies on the Focsani Basin (Matenco et al., 2003; Tarapoanca et al., 2003). Specifically, new and significant contributions of this work are: (1) imaging the full crustal and uppermost mantle (60 km) structure over ~70 km in the Focsani Basin, in the close proximity of the Vrancea Area (~50 km); (2) providing an interpreted depth model for the study area and integrating this model with previous work on a lithosphere scale cross section traversing the East Carpathian Orogen, Vrancea Seismogenic Zone, and Focsani Basin; (3) showing, for the first time, evidence for a slightly east-dipping Moho in the vicinity of VSZ that correlates with thickening of the sedimentary cover towards VSZ (~14 km); thus (4) resulting in thinning of the crust towards the Carpathian orogen which appears to be inconsistent with proposed models westward oceanic lithosphere subduction; and (5) a lack of notable west-dipping structures in the crust and across the Moho, expected from westward subduction.

Based on the position of the SE Carpathian orogen relative to the study area, one would expect a westward thickening of the foreland crust to account for the orogenic root. Correlation of our proposed tectonic model with the earthquake hypocenters, (Fig. 7) shows that a dramatic and unlikely bending of the crust would be required in order to sustain the "subduction in place" hypothesis. While our conclusions challenge the "subduction in place" hypothesis, they do not necessarily prove the alternative "continental delamination" hypothesis and this is not the scope of the paper. In the absence of other mechanisms to generate mantle seismicity, this work only favors continental lithospheric delamination versus oceanic lithosphere subduction to be responsible for the Vrancea intermediate-depth seismicity.

Acknowledgements

Many thanks are due to the Romania State Oil Company "Prospectiuni S.A." for releasing the seismic data to USC. Acknowledgment is made to the donors of The Petroleum Research Fund, administered by the ACS, for partial support of this research. This study was initiated with funds from the COBASE program of the National Research Council, and supported in part by NSF grant EAR-0310118 from the Tectonics Program. We thank Liviu Matenco for providing us with a comprehensive GIS database. Our work has benefited significantly from discussions with V. Mocanu, L. Matenco, V. Raileanu, and R. Trenkamp. We thank Dr. Randell Stephenson and an anonymous reviewer for comments that helped improve the manuscript. Processing of the seismic data was supported by an educational grant from Landmark Graphics Corporation.

References

Artyushkov, E.V., Baer, M.A., Moerner, N.A., 1996. The East Carpathians; indications of phase transitions, lithospheric failure and decoupled evolution of thrust belt and its foreland. Tectonophysics 262, 101–132.

Barnes, A.E., 1994. Moho reflectivity and seismic signal penetration. Tectonophysics 232 (1–4), 299–307.

Bird, P., 1979. Continental delamination and the Colorado Plateau. Journal of Geophysical Research 84 (B13), 7561–7571.

Burchfiel, B.C., 1976. Geology of Romania. Geological Society of America, Special Paper 158. 82 pp.

Cloething, S., Ziegler, P.A., Beekman, F., Andriessen, P.A.M., Matenco, L., Bada, G., Garcia-Castellanos, D., Hardebol, N., Dezes, P., Sokoutis, D., 2005. Lithospheric memory, state of stress and rheology: neotectonic controls on Europe's intraplate continental topography. Quaternary Science Reviews 24, 241–304.

Cornea, I., Radulescu, F., Pompilian, A., Sova, A., 1981. Deep seismic sounding in Romania. Pure and Applied Geophysics (Electronic Ed.) 119, 1144–1156.

Csontos, L., Voros, A., 2004. Mesozoic plate tectonic reconstruction of the Carpathian region. Palaeogeography, Palaeoclimatology, Palaeoecology 210, 1–56.

Ellouz, N., Roca, E., 1994. Palinspastic reconstructions of the Carpathians and adjacent areas since the Cretaceous: a quantitative approach. In: Roure, F. (Ed.), Peri-Tethyan Platforms. Editions Technip, Paris, pp. 51–78.

Enescu, D., Cornea, I., Constantinescu, P., Radulescu, Fl., Patrut, St., 1972. Structura scoartei terestre si a mantalei superioare in zona curburii Carpatilor. Studii si Cercetari de Geologie, Geofizica, Geografie, Seria Geofizica 1 (10).

Girbacea, R., Frisch, W., 1998. Slab in the wrong place: lower lithospheric mantle delamination in the last stage of the Eastern Carpathian subduction retreat. Geology 26, 611–614.

Gvirtzman, Z., 2002. Partial detachment of a lithospheric root under the southeast Carpathians: toward a better definition of the detachment concept. Geology 30, 51–54.

Hauser, F., Raileanu, V., Fielitz, W., Bala, A., Prodehl, C., Polonic, G., Schulze, A., 2001. VRANCEA99—the crustal structure beneath the southeastern Carpathians and the Moesian Platform from a seismic refraction profile in Romania. Tectonophysics 340, 233–256.

Isacks, B., Oliver, J., Skyes, L.R., 1968. Seismology and the new global tectonics. Journal of Geophysical Research 73, 5855–5899.

Knapp, C.C., Knapp, J.H., Raileanu, V., Matenco, L., Mocanu, V., Stephenson, R., Mucuta, D.M., Dinu, C., 2003. Mechanical Coupling of Southeastern Carpathian Foreland Deformation with Vrancea Mantle Seismicity, the 4th Stephan Mueller Conference, Romania.

Knapp, C.C., Knapp, H.J., Connor, J.A., 2004. Crustal-scale structure of the South Caspian Basin revealed by deep seismic reflection profiling. Marine and Petroleum Geology 21, 1073–1081.

Knapp, H.J., Knapp, C.C., Raileanu, V., Matenco, L., Mocanu, V., Dinu, C., 2005. Crustal constraints on the origin of mantle seismicity in the Vrancea Zone, Romania: the case for active continental delamination. Tectonophysics 410, 311–323.

Linzer, H.-G., 1996. Kinematics of retreating subduction along the Carpathian arc, Romania. Geology 24, 167–170.

Linzer, H.-G., et al., 1998. Kinematic evolution of the Romanian Carpathians. Tectonophysics 297, 133–156.

Mason, P.R.D., Seghedi, I., Szakacs, A., Downes, H., 1998. Magmatic constraints on geodynamic models of subduction in the East Carpathains, Romania. Tectonophysics 297, 157–176.

Matenco, L.C., 1997. Tectonic evolution of the outer Romanian Carpathians, PhD thesis, Faculty of Earth Sciences, The Netherlands.

Matenco, L., Bertotti, G., 2000. Tertiary tectonic evolution of the external East Carpathians (Romania). Tectonophysics 316 (3–4), 255–286.

Matenco, L., Bertotti, G., Cloething, S., Dinu, C., 2003. Subsidence analysis and tectonic evolution of the external Carpathian–Moesian Platform region during Neogene times. Sedimentary Geology 156 (1–4), 71–94.

Mohorovicic, A., 1910. Das Beben vom 8. X. 1909: Jahrbuch des Meteorologischen Observatoriums in Zagreb (Agram) fur das Jahr 1909, Jahrgang 9, Teil 4, Abschnitt 1, pp. 3–63.

Oncescu, M.C., Bonjer, K.P., 1997. A note on the depth recurrence and strain release of large Vrancea earthquakes. Tectonophysics 272, 291–302.

Panea, I., Stephenson, R., Knapp, C., Mocanu, V., Drijkoningen, G., Matenco, L., Knapp, J., Prodehl, K., 2005. Near-vertical seismic reflection image using a novel acquisition technique across the Vrancea Zone and Focsani Basin, south-eastern Carpathians (Romania), Cheile Buti Stefan Muller Conference. Tectonophysics 410, 293–309.

Pompilian, A., Radulescu, Fl., Diaconescu, M., Biter, M., Bala, A., 1993. Refraction seismic data in the eastern side of Romania. Romanian Reports in Physics 45 (7–8), 613–621.

Radulescu, F., 1988. Seismic models of the crustal structure of Romania. Revista Romania de Geologie, Geophysica et Geographie 32.

Radulescu, D., Cornea, I., Sandulescu, M., Constantinescu, P., Radulescu, F., Pompilian, A., 1976. Structure de la croute terrestre en Roumanie, essai d'interpretation des etudes sismiques profondes. Anuarul Institutului de Geologie si Geofizica L (in French).

Radulescu, F., Constantinescu, P., Pompilian, A., Ibadof, N., Sova, A., 1979. Structura scoartei terestre pe profilul Galati–Oradea, determinate prin cercetari geofizice, Studii si cercetari de geofizica aplicata, Seria D, Nr. 12 (in Romanian).

Radulescu, F., Mocanu, V., Nacu, V., Diaconescu, C., 1996. Study of recent crustal movements in Romania: a review. J. Geodynamics 22 (1/2), 33–50.

Raileanu, V., Diaconescu, C.C., 1998. Some seismic signatures in the Romanian lithosphere. Tectonophysics 288, 127–136.

Raileanu, V., Diaconescu, C.C., Radulescu, F., 1994. Characteristics of Romanian lithosphere from deep seismic reflection profiling. Tectonophysics 239, 165–185.

Raileanu, V., Hauser, F., Fielitz, W., Dinu, C., Bala, A., Landes, M., Prodehl, C., 2005. A crustal structure model from the North Dobrogea through the Vrancea region to the Western Transylvania. Journal of the Balkan Geophysical Society 8 (Suppl. 1), 299–302.

Royden, L.H., 1993. The tectonic expression of slab pull at continental convergent boundaries. Tectonics 12 (2), 303–325.

Sandulescu, M., 1984. Geotectonica Romaniei (Geotectonics of Romania). Ed. Tehnica, Bucharest. 450 pp. (in Romanian).

Sandulescu, M., 1988. Cenozoic tectonic history of the Carpathians. In: Royden, L.H., Horvath, F. (Eds.), The Pannonian Basin, A Study in Basin Evolution. AAPG Memoir, vol. 45, pp. 17–25.

Stoffa, P.L., Buhl, P., Diebold, J.B., Wenzel, F., 1981. Direct mapping of seismic data to the domain of intercept time and ray parameter: a plane-wave decomposition. Geophysics 46, 255–267.

Szakacs, A., Seghedi, I., Ioane, D., Pecskay, Z., Rogobete, M., 1995. Time-space evolution and magma production rates in the Calimani–Gurghiu–Harghita volcanic chains (East Carpathians, Romania), X-th RCMNS Congress, Bucharest, Abstract volume 2. Romanian Journal of Stratigraphy 76 (7), 55–56 (Suppl.).

Taner, M.T., O'Doherty, R.F., Baysal, E., 1991. Multiple suppression by multi-channel predictive deconvolution. Technical Programme

and Abstracts of Papers—European Association of Exploration Geophysicists 53, 22–23.
Tarapoanca, M., Bertotti, G., Matenco, L., Dinu, C., Cloetingh, S.A.P.L., 2003. Architecture of the Focsani Depression: a 13 km deep basin in the Carpathians bend zone (Romania). Tectonics 22 (6).
Wortel, M.J.R., Spakman, W., 2000. Subduction and slab detachment in the Mediterranean–Carpathian region. Science 290 (5498), 1910–1917.
Yilmaz, O., 1987. Seismic Data Processing. SEG, pp. 241–353.